Nine-Vertex Polyhedral Monothiaborane Chemistry: Synthesis, Molecular Structures, and NMR Characterization of the New Thianonaboranes *exo*-6-L-*arachno*-4-SB_8H_{10}[1a]

Josef Holub,[1b] Bohumil Štíbr,*,[1b] John D. Kennedy,[1c] Mark Thornton-Pett,*,[1c,d] Tomáš Jelínek,[1b] and Jaromír Plešek[1b]

Institute of Inorganic Chemistry, Academy of Sciences of the Czech Republic, 250 68 Řež, Czech Republic, and School of Chemistry, University of Leeds, Leeds LS2 9JT, U.K.

Received February 11, 1994[⊗]

Reactions between *arachno*-4-SB_8H_{12} (**1**) and Lewis bases L in benzene or without solvent generate a series of the corresponding *exo*-6-L-*arachno*-4-SB_8H_{10} (**2**) compounds [L = SMe_2 (**2a**), PPh_3 (**2b**), MeCN (**2c**), NMe_3 (**2d**), pyridine (py) (**2e**), urotropine (uro) (**2f**)], and a bidentate-ligand adduct *exo,exo'*-6,6'-(uro)-(*arachno*-4-SB_8H_{10})$_2$ (**2g**) has also been isolated. Compound **2d** has also been prepared by a ligand displacement reaction between **2a** and trimethylamine, and similar adducts with L = MeNC and quinoline (quin) (**2h, 2i**) were isolated as side products from the reactions between *nido*-6-SB_9H_{11} (**3**) and corresponding Lewis bases. All these compounds are characterized by mass spectrometry and ^{11}B and ^1H NMR spectroscopy. Single-crystal X-ray diffraction studies have been carried out on three representatives of the series, viz. those with L = uro (**2f**), $^1/_2$ uro (**2g**), and MeNC (**2h**). Crystal data for **2f** (at 200 K): mol wt 268.9; monoclinic; space group $C2/c$; $Z = 8$; $a = 2064.16(9)$, $b = 680.85(5)$, $c = 2061.61(12)$ pm; $\beta = 104.467(5)°$; $R = 0.0647$; $R_w = 0.0743$. Crystal data for **2g** (at 200 K): mol wt 397.6; monoclinic; space group $P2_1/c$; $Z = 4$; $a = 1228.24(8)$, $b = 1296.79(8)$, $c = 1452.62(10)$ pm; $\beta = 110.394(4)°$; $R = 0.046$; $R_w = 0.0543$. Crystal data for **2h** (at 200 K): mol wt 169.8; monoclinic; space group $P2_1/m$; $Z = 2$; $a = 557.93(8)$, $b = 909.36(9)$, $c = 987.16(11)$ pm; $R = 0.0377$; $R_w = 0.0436$.

Introduction

Our two groups have a continuing and developing interest in the synthesis, NMR properties, structural characterization, and reactions of the group 15 and 16 polyhedral heteroboranes,[2] with special emphasis so far on the azaborane[2-6] and thiaborane[5,7-10] families, and we have reported on *arachno*-4-NB_8H_{13},[3,5] *nido*-6-NB_9H_{12},[4,5] 9-L-*arachno*-6-NB_9H_{12} (where L = H, SMe_2, MeCN, and PPh_3),[4,5] *arachno*-6,9-$N_2B_8H_{12}$,[6] *arachno*-4-SB_8H_{12},[5,7,8] *nido*-6-SB_9H_{11},[9] and the [*arachno*-6-SB_9H_{12}]$^-$ anion.[9]

A key compound for the further development of nine-vertex *arachno* heteroborane chemistry is *arachno*-4-thianonaborane, 4-SB_8H_{12} (compound **1**). This compound was first isolated almost two decades ago[10] but was supposed initially to be *nido*-SB_8H_{10}. Subsequently, one of our groups developed an alternative synthesis and deduced its correct formulation;[7] more recently we reported a convenient high-yield synthesis[8] that makes this thiaborane one of the most accessible thiaborane synthons. Except for deprotonation to give the [*arachno*-4-SB_8H_{11}]$^-$ anion,[8] no nonmetallic chemistry of compound **1** has so far been reported. We have therefore developed this area somewhat by exploring the reactions of compound **1** with Lewis bases. This work has led to the isolation of a family of compounds of general constitution *exo*-6-L-*arachno*-4-SB_8H_{10} (**2**), which we now describe in this paper.

Table 1. Properties of the Products from Reactions between-*arachno*-4-SB_8H_{12} (**1**) and Lewis Bases

base	ratio[a]	time, days	product	yield, %	R_f (benzene)	mp, °C	m/z_{max}
SMe_2[b]	10	3	**2a**	86	0.53	73	192
PPh_3	1.05	4	**2b**	73	0.75	178	382
MeCN[b]	15	3	**2c**	64	0.37	130	171
NMe_3	5	2	**2d**	79	0.42	145	153
py	1.05	2	**2e**	63	0.50	106	209
uro	1.4	4	**2f**	31	0.56[c]	175	270
			2g	18	0.08[c]	183	400

[a] Molar ratio base/SB_8H_{12}. [b] Reaction carried out without solvent. [c] In dichloromethane.

Experimental Section

General Procedures. Unless otherwise stated, all reactions were carried out under nitrogen though some subsequent operations, e.g., analytical thin-layer chromatography (TLC), preparative TLC, and column chromatography, were carried out in air. The thiaboranes 4-SB_8H_{12} and 6-SB_9H_{11} and methyl isocyanide were prepared by literature methods.[8,11,12] Hexane, dichloromethane, and benzene were distilled from calcium hydride, chloroform and acetonitrile were distilled from P_4O_{10}, and dimethyl sulfide was distilled from solid potassium hydroxide prior to use. Other chemicals were of reagent or analytical

---

[⊗] Abstract published in *Advance ACS Abstracts,* August 1, 1994.

[1] (a) Contribution No. 31 from the Anglo-Czech polyhedral collaboration (ACPC) between the Institute of Inorganic Chemistry, Academy of Sciences of the Czech Republic, and School of Chemistry, University of Leeds. (b) Academy of Sciences of the Czech Republic. (c) University of Leeds. (d) To whom crystallographic queries should be addressed.

[2] Štíbr, B.; Plešek, J.; Heřmánek, S. In *Advances in Boron and the Boranes*; Liebman, J. E., Greenberg, A., Williams, R. E., Eds.; VCH Publishers: New York, 1988; pp 35–70 and references therein.

[3] Baše, K.; Plešek, J.; Heřmánek, S.; Huffman, J.; Ragatz, P.; Schaeffer, R. *J. Chem. Soc., Chem. Commun.* **1975**, 934.

[4] Baše, K.; Hanousek, F.; Štíbr, B.; Plešek, J.; Lyčka, J. J. *J. Chem. Soc., Chem. Commun.* **1981**, 1162.

[5] Baše, K. *Collect. Czech. Chem. Commun.* **1983**, *48*, 2593.

[6] Štíbr, B.; Kennedy, J. D.; Jelínek, T. *J. Chem. Soc., Chem. Commun.* **1990**, 1309.

[7] Baše, K.; Gregor, V.; Heřmánek, S. *Chem. Ind. (London)* **1979**, 743.

[8] Baše, K.; Wallbridge, M. G. H.; Fontaine, X. L. R.; Greenwood, N. N.; Jones, J. H.; Kennedy, J. D.; Štíbr, B. *Polyhedron* **1989**, *8*, 2089.

[9] Bown, M.; Fontaine, X. L. R.; Kennedy, J. D. *J. Chem. Soc., Dalton Trans.* **1988**, 1467.

[10] Pretzer, W. R.; Rudolph, R. W. *J. Am. Chem. Soc.* **1976**, *98*, 1441.

[11] Rudolph, R. W.; Pretzer, W. R. *Inorg. Synth.* **1983**, *22*, 226.

[12] Casanova, J., Jr.; Schuster, R. E.; Werner, N. D. *J. Chem. Soc.* **1963**, 4280.

Table 2. Crystal Data and Structure Solution and Refinement Parameters[a] for *exo*-6-L-*arachno*-4-SB_8H_{10} Compounds [L = uro (**2f**), 1/2 uro (**2g**), MeNC (**2h**)]

	2f	2g	2h
formula	$C_6H_{22}B_8N_4S$	$C_6H_{32}B_{16}N_4S_2$	$C_2H_{13}B_8NS$
size, mm^3	0.6 × 0.4 × 0.2	0.6 × 0.35 × 0.2	0.13 × 0.17 × 0.69
mol wt	268.82	397.46	169.69
crystal system	monoclinic	monoclinic	monoclinic
space group	*C2/c*	*P2₁/c*	*P2₁/m*
a, pm	2064.16(9)	1228.24(8)	557.93(8)
b, pm	680.85(5)	1296.79(8)	909.36(9)
c, pm	2061.61(12)	1452.62(10)	987.16(11)
β, deg	104.467(5)	110.394(4)	90.399(9)
V, nm^3	2.8055(3)	2.1687	0.50083(10)
D_c, g cm^{-3}	1.27	1.22	1.13
Z	8	4	2
μ, cm^{-1}	17.68	21.43	22.27
no. of data collected	2277	3400	1536[b]
no. of obsd data	1973	3071	655
no. of params	201	360	100
weighting param *g*[c]	0.0001	0.0002	0.0001
R	0.0647	0.0446	0.0377
R_w	0.0743	0.0543	0.0436

[a] Common to all three structures: copper Kα radiation (λ = 154.184 pm); 4.0 < 2θ < 120.0°; $\omega-\theta$ scans; each scan divided into 30 steps, scan width and step sizes calculated from a learned profile; scan speeds 0.4−1.5° min^{-1}; *T* = 200 K. [b] Two equivalents of data collected. [c] $w = [\sigma^2(F_o) + g(F_o)^2]^{-1}$.

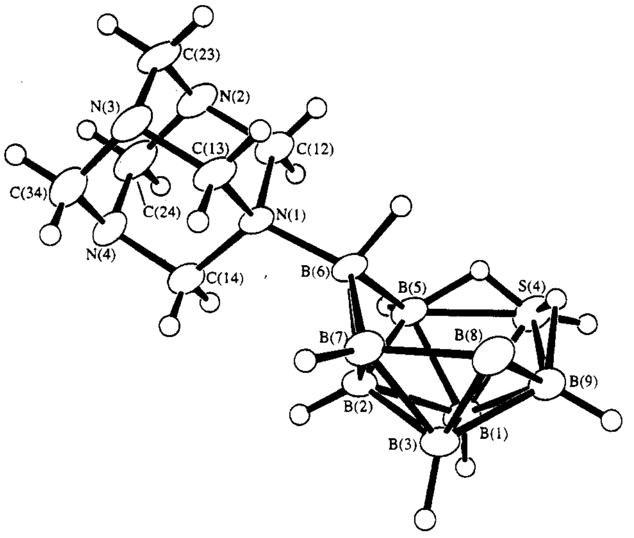

Figure 1. Perspective drawing of the molecular structure of *exo*-6-(uro)-*arachno*-4-SB_8H_{10} (**2f**).

grade and were used as purchased. All evaporations of solvents were carried out using standard rotary evaporation techniques, and vacuum filtrations were performed using a Schlenk apparatus. Column chromatography was performed using silica gel of standard quality, and preparative TLC was carried out using silica gel (Fluka, type GF 254) as the stationary phase on plates of dimensions 200 × 200 × 1 mm,[3] made on glass formers from aqueous slurries followed by drying in air at 80 °C. The purity of individual chromatographic fractions was checked by analytical TLC on Silufol (Kavalier, silica gel on aluminum foil; detection by diiodine vapor, followed by 2% aqueous $AgNO_3$ spray).

Physical Measurements. Melting points were measured in sealed capillaries under nitrogen and are uncorrected. Low-resolution mass spectra were obtained using a JEOL HP-5985 instrument (70 eV EI, FAB, and CI ionization). Proton (^1H) and boron (^{11}B) NMR spectra were recorded at 2.35 and 9.4 T on JEOL FX100 and Bruker AM 400 instruments, respectively. The [$^{11}B-^{11}B$] COSY and $^1H\{^{11}B(\text{selective})\}$ NMR experiments were essentially as described in other recent papers from our laboratories.[13,14] Chemical shifts are given in ppm to high-frequency (low field) of Ξ = 32.083 971 MHz (nominally $F_3B{\cdot}OEt_2$ in $CDCl_3$) for ^{11}B (quoted ±0.5 ppm) and Ξ = 100 MHz ($SiMe_4$) for ^1H (quoted ±0.05 ppm), Ξ being defined as in ref 15. Solvent resonances were used as internal secondary standards. Coupling constants $^1J(^{11}B-^1H)$ are taken from resolution-enhanced ^{11}B spectra with digital resolution of 8 Hz and are given in hertz.

General Synthesis of *exo*-6-L-*arachno*-4-SB_8H_{10} (2a−g) Compounds from *arachno*-4-SB_8H_{12} (1). In a typical experiment, a mixture of compound **1** (130 mg; 1 mmol) and excess Lewis base (see Table 1) was dissolved in benzene (10 mL), and the solution was left to stand for 2−4 days (see Table 1) at ambient temperature (dihydrogen evolution). The volatile components were then evaporated, and the solid residue subjected to column (ca. 2.5 cm × 30 cm) chromatography or preparative TLC on silica gel using benzene or dichloromethane (for L = uro) as the liquid phase. The main fractions of R_f(anal.) as in Table 1 were collected, evaporated to dryness, and crystallized from a concentrated solution in dichloromethane that was overlayered by a

Chart 1

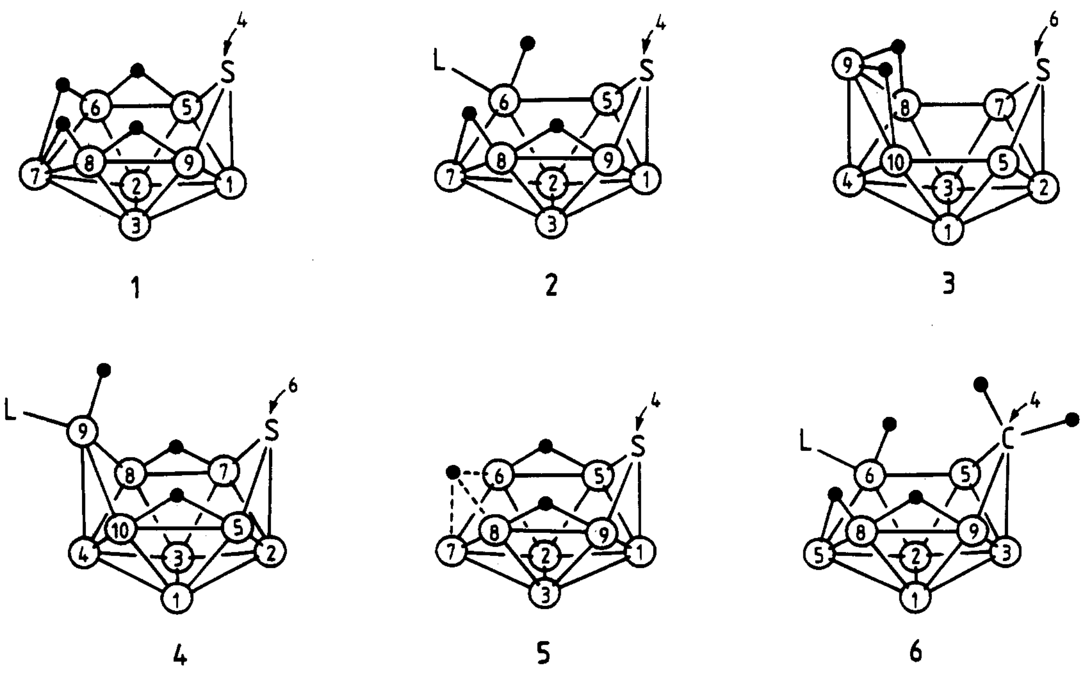

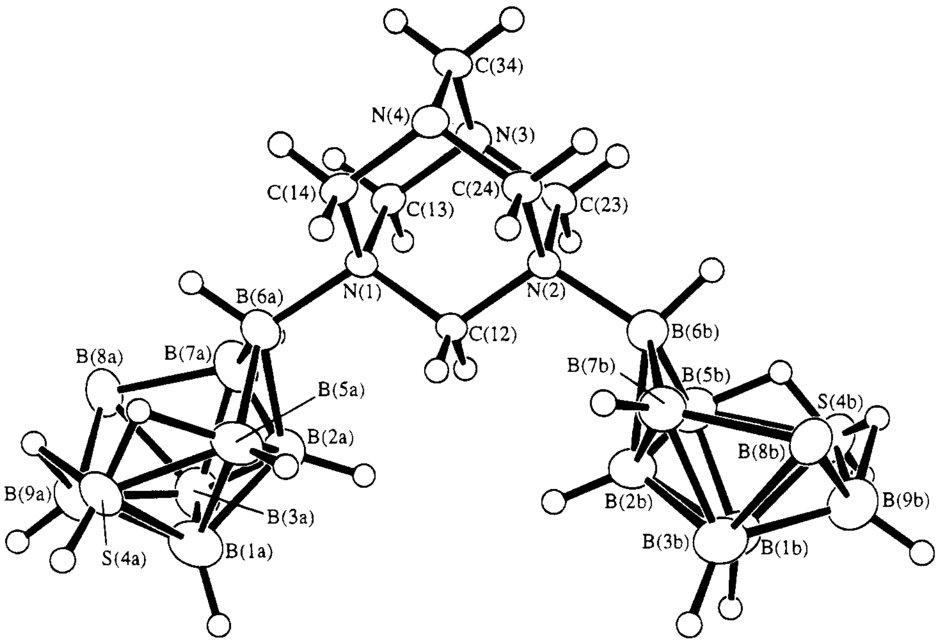

Figure 2. Perspective drawing of the molecular structure of *exo,exo'*-6-(uro)-*arachno*-(4-SB_8H_{10})$_2$ (**2g**).

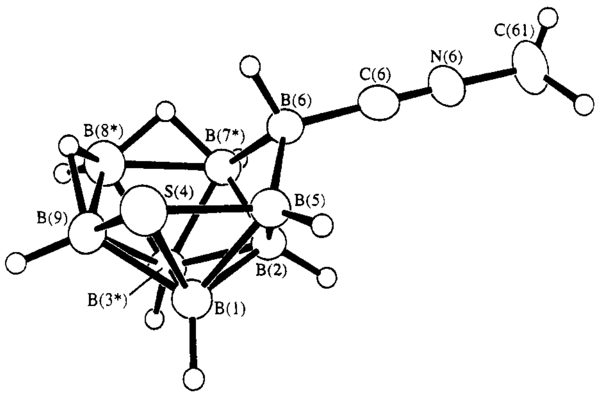

Figure 3. Perspective drawing of the molecular structure of *exo*-6-(MeNC)-*arachno*-4-SB_8H_{10} (**2h**).

2-fold amount of hexane. This yielded crystals (for yields see Table 1) which were identified as *exo*-6-L-*arachno*-4-SB_8H_{10} (**2**) compounds by NMR spectroscopy, mass spectrometry, and X-ray crystallography as described below. Analytical products were obtained by repeated crystallization. For other characteristics of individual compounds see Table 1.

General Synthesis of *exo*-6-L-*arachno*-4-SB_8H_{10} (2h,i) Compounds from *nido*-6-SB_9H_{11} (3). In a typical experiment, a solution of MeNC or quin (7 mmol) in benzene or dichloromethane (15 mL) was added dropwise to a solution of *nido*-6-SB_9H_{11} (3) (141 mg; 1 mmol) in benzene or dichloromethane (15 mL) over a period of 15 min under magnetic stirring and cooling to 0 °C (bath). The mixture was then stirred for an additional 12 h at ambient temperature, the volatile materials were evaporated, and the residue was extracted with three 10-mL portions of 10% aqueous sodium hydroxide (this operation is omitted for L = quin). The insoluble material was dried at ambient temperature (oil pump) and extracted with dichloromethane (*ca.* 20 mL). The dichloromethane extracts were then subjected to chromatography on a TLC plate, using 33% hexane in dichloromethane as the liquid phase to give two main fractions of R_f(prep) 0.30 and 0.24 (for L = MeNC) and 0.20 and 0.28 (for L = quin); these were detected by $AgNO_3$ spray in narrow bands of the silica and extracted with dichloromethane. Individual fractions yielded crystalline compounds which were identified as *exo*-6-L-*arachno*-4-SB_8H_{10} (**2h,i**) by NMR spectroscopy and X-ray crystallography as described below. Analytical products **2h** [50 mg, 21%; m/z_{max} 171 (M^+)] and **2i** [39 mg, 15%; m/z_{max} 259 (M^+)] were obtained from concentrated dichloromethane solutions that were overlayered by a 2-fold volume of hexane. Identical workup of the latter TLC fractions gave crystals (yields 32 and 63%, respectively) which were identified as *exo*-9-L-*arachno*-4-SB_9H_{11} (**4**) (where L = MeNC or quin) by NMR spectroscopy, mass spectrometry, and X-ray crystallography as will be reported elsewhere.[16]

X-ray Data Collection and Structure Determination and Refinement. Crystals of **2f–h** suitable for single-crystal X-ray diffraction studies were obtained as described in the preceding paragraphs. All crystallographic measurements were made at 200 K on a Stoe STADI4 diffractometer operating in the $\omega-\theta$ scan mode using Cu Kα radiation (λ = 154.184 pm) and an on-line profile fitting method.[17] The structures of all three compounds were determined using SHELXS86[18] and were determined by full-matrix least-squares procedures using SHELX76.[19] All three compounds crystallize as racemic mixtures of two enantiomers (the mixture of **2g** also includes a *meso* isomer), so that in all three cases the cage sulfur atom is disordered over the 4- and 8-positions. In the case of **2h**, which possesses a crystallographic mirror plane passing through the non-hydrogen atoms of the MeNC substituent, B(6), B(2), and B(9), this disorder must be exactly 50/50; refinement of a population parameter for the sulfur atom(s) for both **2f** and **2g** resulted in a very similar ratio for both of these complexes. The disorder was therefore treated by refining the 4-position (for **2h**) or the 4- and 8-positions (for **2f** and **2g**) as a boron atom and a sulfur atom each with half-occupancy factors and the same positional and thermal parameters. In all three cases all non-hydrogen atoms, including those of the disordered 4- and 8-vertices, were refined with anisotropic thermal parameters.

A further result of the disorder of the cluster sulfur atom is a set of halfoccupancy hydrogen atoms: two *exo*-terminal (in the 4- and 8-positions) and four bridging [across the (4,5)-, (4,9)-, (7,8)-, and (8,9)-edges]. In all three cases these half-occupancy atoms were readily apparent on Fourier difference maps. The methyl hydrogen atoms of **2f** and **2g** were included in calculated positions (C–H = 96 pm) and were refined with an overall isotropic thermal parameter. All other hydrogen atoms were located on Fourier difference maps and were freely refined with isotropic thermal parameters, part from the half-

---

(13) Plešek, J.; Štíbr, B.; Fontaine, X. L. R.; Kennedy, J. D.; Heřmánek, S.; Jelínek, T. *Collect. Czech. Chem. Commun.* **1991**, *56*, 1618.

(14) Fontaine, X. L. R.; Kennedy, J. D.; McGrath, M.; Spalding, T. R. *Magn. Reson. Chem.* **1991**, *29*, 711.

(15) McFarlane, W. *Proc. R. Soc. London, Ser. A* **1986**, *306*, 185.

(16) Štíbr, B.; Holub, J.; Jelínek, T.; Kennedy, J. D.; Thornton-Pett, M. Manuscript in preparation.

(17) Clagg, W. *Acta Crystallogr., Sect. A* **1987**, *37*, 22.

(18) Sheldrick, G. M. *Acta Crystallogr., Sect. A* **1990**, *46*, 467.

(19) Sheldrick, G. M. SHELX76: Program System for X-Ray Structure Determination. University of Cambridge, England, 1976.

Table 3. Non-Hydrogen Atomic Coordinates ($\times 10^4$) and Their Equivalent Isotropic Thermal Parameters (pm^2) Together with Cluster Hydrogen Atomic Coordinates ($\times 10^3$) and Their Isotropic Thermal Parameters (pm^2) for *exo*-6-L-*arachno*-4-SB_8H_{10} Compounds [L = uro (**2f**), $^1/_2$ uro (**2g**), MeNC (**2h**)]

atom	x	y	z	U_{iso}/U_{eq}[a]	atom	x	y	z	U_{iso}/U_{eq}[a]
Compound **2f**									
N(1)	3640.2(8)	3284(3)	3781.6(8)	24.0(6)	B(7)	2511.4(13)	5731(4)	3959.3(13)	28.5(9)
N(2)	4604.0(9)	1067(3)	3893.7(10)	35.5(7)	S/B(8)	1903.4(5)	5683(2)	4514.0.0(5)	30.6(4)
N(3)	4788.6(9)	4549(3)	4150.6(10)	34.0(7)	B(9)	1346.5(12)	3622(4)	4122.9(13)	27.5(8)
N(4)	4352.8(9)	3488(3)	2995.7(9)	37.1(7)	H(1)	110.1(11)	263(4)	284.8(12)	38(7)
C(12)	3926.7(11)	1238(3)	3968.5(12)	31.6(8)	H(2)	234.5(11)	457(3)	283.2(11)	33(6)
C(13)	4114.6(10)	4727(4)	4232.7(11)	30.8(8)	H(3)	133.0(13)	653(4)	325.4(12)	51(7)
C(14)	3671.7(11)	3686(4)	3063.3(10)	32.8(8)	H(5)	236.9(11)	46(4)	319.6(11)	33(6)
C(23)	5022.3(10)	2529(4)	4328.2(12)	36.4(8)	H(6)	297.7(10)	284(4)	449.2(11)	32(6)
C(24)	4602.2(12)	1497(4)	3194.5(12)	42.9(10)	H(7)	274.6(11)	713(4)	392.0(10)	34(6)
C(34)	4780.3(12)	4905(4)	3446.1(12)	41.9(10)	H(9)	84.7(10)	369(3)	419.3(10)	28(6)
B(1)	1483.6(12)	2920(4)	3299.5(12)	28.6(8)	H(4)	1228	24	3860	50
B(2)	2236.3(12)	4115(4)	3290.8(12)	27.5(9)	H(8)[b]	1663	6968	4755	50
B(3)	1623.3(12)	5410(4)	3585.7(12)	28.5(9)	H(45)[b]	2154	1201	4215	50
S/B(4)	1638.3(4)	1083.2(12)	4020.3(4)	32.1(3)	H(49)[b]	1730	2197	4523	50
B(5)	2285.2(12)	1660(4)	3516.8(12)	28.1(8)	H(78)[b]	2518	5608	4622	50
B(6)	2920.6(11)	3394(4)	3931.6(12)	23.6(8)	H(89)[b]	1758	4176	4714	50
Compound **2g**									
N(1)	2154.7(14)	2488.5(12)	1231.3(12)	20.6(6)	B(9b)	−3452(2)	1072(2)	1186(2)	34.7(9)
N(2)	22(2)	2517.9(13)	619.1(12)	20.6(6)	H(1a)	369(2)	−14(2)	399(2)	56(2)
N(3)	1114.3(14)	4075.3(13)	554.6(12)	24.3(5)	H(2a)	235(2)	163(2)	320(2)	45(2)
N(4)	1070(2)	2649.5(13)	−530.0(12)	23.7(6)	H(3a)	461(2)	170(2)	490(2)	54(2)
C(12)	1086(2)	2094(2)	1362(2)	21.4(6)	H(4a)	485(2)	−80(2)	292(2)	55(2)
C(13)	2151(2)	3657(2)	1295(2)	23.4(6)	H(5a)	253(2)	15(2)	192(2)	46(2)
C(14)	2093(2)	2212(2)	188(2)	23.6(7)	H(6a)	403(2)	206(2)	171(2)	50(2)
C(23)	86(2)	3691(2)	702(2)	22.9(7)	H(7a)	393(2)	345(2)	335(2)	57(2)
C(24)	35(2)	2245(2)	−403(2)	24.1(7)	H(8a)	637(2)	241(2)	413(2)	49(2)
C(34)	1092(2)	3778(2)	−435(2)	26.5(7)	H(9a)	623(2)	43(2)	426(2)	47(2)
B(1a)	4017(3)	426(2)	3575(2)	40.8(8)	H(45a)	420(2)	40(2)	202(2)	50(2)
B(2a)	3233(2)	1565(2)	3121(2)	29.3(8)	H(49a)	555(2)	42(2)	284(2)	47(2)
B(3a)	4512(2)	1636(3)	4135(2)	38.1(8)	H(78a)	495(2)	251(2)	307(2)	48(2)
S/B(4a)	4618.6(13)	−118.8(11)	2684.3(10)	42.2(5)	H(89a)	589(2)	155(2)	337(2)	52(2)
B(5a)	3266(3)	621(2)	2263(2)	31.6(8)	H(1b)	−195(2)	110(2)	300(2)	40(2)
B(6a)	3325(2)	1979(2)	1997(2)	23.8(7)	H(2b)	−14(2)	93(2)	213(2)	38(2)
B(7a)	4090(2)	2619(2)	3163(2)	35.1(8)	H(3b)	−189(2)	−57(2)	168(2)	45(2)
S/B(8a)	5692.5(7)	2258.8(7)	3715.6(6)	39.0(3)	H(4b)	−337(2)	269(2)	225(2)	50(2)
B(9a)	5516(3)	773(2)	3764(2)	36.8(8)	H(5b)	−91(2)	300(2)	239(2)	51(2)
B(1b)	−2074(2)	1317(2)	2227(2)	35.1(8)	H(6b)	−182(2)	256(2)	17(2)	50(2)
B(2b)	−1008(2)	1214(2)	1675(2)	29.2(7)	H(7b)	−107(2)	25(2)	13(2)	43(2)
B(3b)	−2126(2)	282(2)	1382(2)	35.1(9)	H(8b)	−372(2)	−13(2)	−24(2)	43(2)
S/B(4b)	−3089.9(10)	2435.8(9)	1652.9(8)	40.9(4)	H(9b)	−419(2)	84(2)	132(2)	52(2)
B(5b)	−1472(3)	2445(2)	1828(2)	31.6(8)	H(45b)	−251(2)	279(2)	133(2)	44(2)
B(6b)	−1156(2)	2109(2)	731(2)	22.7(7)	H(49b)	−366(2)	207(2)	95(2)	49(2)
B(7b)	−1555(2)	770(2)	462(2)	27.5(7)	H(78b)	−257(2)	96(2)	−10(2)	49(2)
S/B(8b)	−3149.9(8)	500.2(8)	98.2(7)	33.5(4)	H(89b)	−359(2)	110(2)	24(2)	49(2)
Compound **2h**									
B(1)	−2698(4)	1511(2)	3182(2)	34.1(7)	H(1)	−392(4)	88(2)	389(2)	53(6)
B(2)	−3606(5)	2500[a]	1732(3)	32.3(9)	H(2)	−554(6)	250[a]	137(3)	53(8)
S(4)	354(2)	680.2(9)	2889.5(8)	42.8(4)	H(5)	−261(3)	−12(2)	112(2)	48(5)
B(5)	−1960(4)	887(2)	1473(2)	34.2(7)	H(6)	39(5)	250[a]	29(3)	47(8)
B(6)	−1493(5)	2500[a]	424(3)	33.1(10)	H(8)	55(7)	530(4)	351(4)	47(10)
C(6)	−2812(5)	2500[a]	−949(3)	34.4(9)	H(9)	74(5)	250[a]	484(3)	45(7)
N(6)	−3797(4)	2500[a]	−1966(2)	36.5(8)	H(78)	24(8)	63(5)	162(5)	70(14)
C(61)	−5077(7)	2500[a]	−3227(3)	48.5(11)	H(89)	176(6)	340(3)	314(3)	24(8)
B(9)	48(5)	2500[a]	3749(3)	38.0(11)	H(61a)	−499(5)	163(3)	−363(3)	86(8)
					H(61b)	−690(9)	250[a]	−315(5)	136(20)

[a] $U_{eq} = {}^1/_3 \times$ trace of the normalized $\mathbf{U}_{ij}$ tensor. [b] Parameters were not refined for these atoms. [c] Coordinate fixed because atom is on a special position.

occupancy hydrogen atoms of **2f**, which were not refined because they tended to move to unreasonable positions. The weighting scheme $w = [\sigma^2(F_o) + g(F_o)^2]^{-1}$ was used in all three cases. Full details of crystal data, data collection, and structure solution and refinement are given in Table 2.

Results and Discussion

Syntheses. We initially observed the formation of compounds with the nine-vertex *exo*-6-L-*arachno*-4-SB_8H_{10} constitution **2** (see Chart 1) in the reactions between ten-vertex *nido*-6-SB_9H_{11} (compound **3**)[11] and Lewis bases, such as methyl isocyanide and quinoline (quin), in benzene or dichloromethane at room temperature. From the products of these reactions we isolated compounds *exo*-6-L-*arachno*-4-SB_8H_{10} (**2h,i**) (yields 21 and 15%, respectively) and corresponding ten-vertex compounds of the *exo*-9-L-*arachno*-6-SB_9H_{11} (**4**) type, *exo*-9-L-*arachno*-4-SB_9H_{11} (**4**) (yields 32 and 63%, respectively). In these cases, compounds of type **2** apparently result from the degradation of the B(9) vertex in structure **3**, followed by or associated with attack by base at the B(5) site. The constitution

Table 4. Selected Cluster Interatomic Distances (pm) for *exo*-6-L-*arachno*-4-SB_8H_{10} Compounds [L = uro (**2f**), ½ uro (**2g**), MeNC (**2h**)]

bond[a]	**2f**	**2g**[b]	**2g**[c]	**2h**[d]
B(2)—B(1)	175.8(6)	176.2(4)	176.2(4)	176.2(5)
B(3)—B(1)	179.5(6)	177.3(4)	180.5(4)	179.9(6)
S/B(4)—B(1)	190.7(5)	184.0(4)	190.5(4)	188.7(7)
B(5)—B(1)	181.8(5)	182.2(4)	182.2(4)	183.0(5)
B(9)—B(1)	185.2(6)	182.0(4)	186.2(4)	185.9(5)
B(3)—B(2)	177.0(6)	174.1(4)	176.5(4)	176.2(5)
B(5)—B(2)	173.2(6)	175.7(4)	173.5(4)	175.1(5)
B(6)—B(2)	174.6(5)	175.9(4)	175.8(4)	175.5(6)
B(7)—B(2)	174.4(6)	171.3(4)	175.0(4)	175.1(5)
B(7)—B(3)	181.5(5)	183.8(4)	182.6(4)	183.0(5)
S/B(8)—B(3)	186.5(5)	193.5(4)	187.2(3)	188.7(4)
B(9)—B(3)	183.1(6)	187.9(4)	186.0(4)	185.9(5)
B(5)—S/B(4)	192.5(5)	183.0(4)	191.4(4)	190.6(4)
B(9)—S/B(4)	186.0(5)	195.1(4)	189.1(4)	186.4(4)
B(6)—B(5)	181.3(5)	181.0(4)	181.9(4)	181.5(5)
S/B(8)—B(7)	189.8(5)	190.7(3)	187.6(3)	190.6(4)
B(9)—S/B(8)	186.5(5)	194.3(4)	189.5(4)	186.8(4)

[a] S/B(4) and S/B(8) refer to mixed boron—sulfur sites which result from a 50/50 disorder of a sulfur atom over the cluster 4- and 8-positions. [b] Distances for subcluster a. [c] Distances for subcluster b. [d] B(1)—B(3), S/B(4)—S/B(8), and B(5)—B(7) pairs are related by a mirror plane at $y = 1/4$.

and structure of compound **2h** were determined unambiguously by X-ray diffraction analysis and NMR spectroscopy as described below. The structural and NMR characterization of compounds of type **4** will be discussed in the context of other compounds of structural type **4** in a separate report.[16]

Following the establishment of a convenient high-yield route to *arachno*-SB_8H_{12} (**1**),[8] we found a more rational and convenient synthesis of compounds of the *exo*-6-L-*arachno*-4-SB_8H_{10} type **2** derived from the reaction between compound **1** and Lewis bases L, with stoichiometry as in eq 1. Using this type of

$$\underset{\mathbf{1}}{SB_8H_{12}} + L \rightarrow \underset{\mathbf{2}}{LSB_8H_{10}} + H_2 \qquad (1)$$

reaction, we have isolated a series of compounds **2a**–**g**, which have the *exo*-6-L-*arachno*-4-SB_8H_{10} formulation **2**, where L = SMe_2 (compound **2a**), L = PPh_3 (compound **2b**), L = MeCN (compound **2c**), L = NMe_3 (compound **2d**), L = pyridine (py) (compound **2e**), and L = hexamethylenetetramine (urotropine = uro) (compound **2f**). From the urotropine reaction we have also isolated *exo,exo'*-6,6'-(uro)-(*arachno*-4-SB_8H_{10})$_2$ (compound **2g**), in which urotropine acts as a bidentate ligand, i.e. monodentate to each of two {4-SB_8H_{10}} residues.

The reactions as in eq 1 were carried out in benzene solution (for L = PPh_3, NMe_3, py, and uro) or without a solvent (SMe_2 and MeCN) at room temperature over a period of 2–4 days. The products were isolated by preparative TLC or column chromatography, using silica gel and benzene or (for L = uro) chloroform as a liquid phase. Purification was then effected by crystallization from dichloromethane/hexane, to give good yields (63–86%). Compound **2d** has been prepared alternatively by a ligand displacement reaction between the dimethyl sulfide derivative **2a** and trimethylamine in benzene over a period of 2 days at room temperature; this suggests that other displacement reactions between **2a** and Lewis bases stronger than SMe_2 may also be feasible. Molecular formulas were confirmed by mass spectrometry, and the general cluster configuration **2** for all compounds **2a**–**i** was confirmed unambiguously by NMR spectroscopy (see below), together with single-crystal X-ray diffraction analysis, to give the molecular structures of compounds **2f**–**2h**.

Some insight into the reaction between compound **1** and the Lewis bases L may be provided by the results of a reaction in an NMR tube between compound **1** and pyridine, carried out in $CDCl_3$ *in cavo inter contos*. In this experiment, the previously characterized [*arachno*-4-SB_8H_{11}]$^-$ anion (compound **5**)[8] was detected as a predominant product by ^{11}B NMR spectroscopy in the initial stages of the reaction (*ca.* 15 min). This observation could be taken to suggest (a) that anion **5** could be an intermediate in the reaction of eq 1, producing compounds of type **2** upon electrophilic attack by the [LH]$^+$ cation at the B(6) site in compound **5** and dehydrogenation as in eq 2.

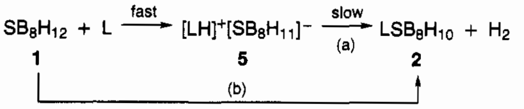

$$\underset{\mathbf{1}}{SB_8H_{12}} + L \xrightarrow{\text{fast}} \underset{\mathbf{5}}{[LH]^+[SB_8H_{11}]^-} \xrightarrow[\text{(a)}]{\text{slow}} \underset{\mathbf{2}}{LSB_8H_{10}} + H_2 \qquad (2)$$

Alternatively (b) the possibility of direct nucleophilic attack on compound **1** itself, which will be in equilibrium with the anion **5** under these conditions, must also be considered.

X-ray Diffraction Studies. The solid-state molecular structures of compounds **2f**–**2h** were determined by single-crystal X-ray diffraction analysis and are depicted in Figures 1–3, respectively. Crystal data and structure solution parameters are given in Table 2 together with details of structure refinement in the Experimental Section; atomic coordinates are listed in Table 3, cluster interatomic distances are given in Table 4, selected angles between interatomic vectors for cluster atoms are listed in Table 5, and selected exocluster bond distances and angles are listed in Table 6.

In all three compounds, the cage sulfur atom is disordered over the 4- and 8-positions (see Experimental Section for details), and this precludes any detailed structural comparisons. The disorder is, however, readily resolved in all three cases, which allows the gross structural features to be identified. Inspection of the structures in Figures 1–3 shows that all three compounds, **2f**–**h**, adopt the same asymmetric *arachno* configuration **2**, which has the sulfur atom at the least-connected cluster 4-position and which has a pair of bridging hydrogen atoms localized at the B(7)—B(8) and B(8)—B(9) bridging positions in the open face. In each case, the ligand moiety is bound to the B(6) atom in an *exo* fashion, the neutral {B(6)-HL} unit thus being isolobal[20] with an anionic {BH_2^-} unit. Hence, the clusters of compounds of type **2** are formally isoelectronic with the parent [*arachno*-4-SB_8H_{11}]$^-$ anion **5**. However, they are not isostructural because the anion exhibits a different arrangement of the extra hydrogen atoms (compare structures **2** and **5**) believed to entail one that has μ-(6,7,8) character, in the open hexagonal face of the cluster.[8]

Intercomparison of equivalent internuclear distances in the clusters of compounds **2f**–**h** in Table 4 reveals surprising similarities, even though ligands such as urotropine and MeNC are quite different. The most significant differences observed in these solid-state structures are in fact associated not directly with the ligand-substituted 6-positions but (a) with the B(7)B(8) and B(8)B(9) pairs of boron atoms that are interconnected by bridging hydrogen atoms and (b) with the boron atoms flanking the S(4) vertex. The asymmetry of the bonding of the H(7,8) and H(8,9) bridging hydrogen atoms is demonstrated by the shorter distances from the B(8) center in all these structures. Comparison of equivalent interatomic distances between the two {6-SB_8H_{10}} subclusters in compound **2g** (see Table 4) shows significant differences in some cases, presumably due to

---

(20) (a) Elian, M.; Hoffmann, R. *Inorg. Chem.* **1975**, *14*, 1058. (b) Hoffmann, R. *Science (Washington, D.C.)* **1981**, *211*, 995.

Table 5. Selected Cluster Bond Angles (deg) for *exo*-6-L-*arachno*-4-SB_8H_{10} Compounds [L = uro (**2f**), $^1/_2$ uro (**2g**), MeNC (**2h**)]

angle[a]	**2f**	**2g**[b]	**2g**[c]	**2h**[d]
B(3)−B(1)−B(2)	59.8(2)	59.0(2)	59.3(2)	59.3(3)
S/B(4)−B(1)−B(2)	109.6(2)	111.1(2)	109.6(2)	109.6(2)
S/B(4)−B(1)−B(3)	112.4(3)	120.3(2)	114.0(2)	113.6(2)
B(5)−B(1)−B(2)	57.9(2)	58.7(2)	57.9(2)	58.3(2)
B(5)−B(1)−B(3)	107.7(3)	108.9(2)	107.6(2)	108.1(2)
B(5)−B(1)−S/B(4)	62.2(2)	60.0(2)	61.7(2)	61.7(2)
B(9)−B(1)−B(2)	103.2(3)	104.0(2)	103.1(2)	103.2(2)
B(9)−B(1)−B(3)	60.2(2)	63.0(2)	61.0(2)	61.1(2)
B(9)−B(1)−S/B(4)	59.3(2)	64.4(2)	60.2(2)	59.8(2)
B(9)−B(1)−B(5)	103.5(3)	103.9(2)	103.5(2)	103.7(3)
B(3)−B(2)−B(1)	61.2(3)	60.8(2)	61.5(2)	61.4(3)
B(5)−B(2)−B(1)	62.8(2)	62.4(2)	62.8(2)	62.8(2)
B(5)−B(2)−B(3)	112.8(3)	113.5(2)	113.5(2)	113.5(3)
B(6)−B(2)−B(1)	114.3(3)	113.6(2)	114.4(2)	114.0(3)
B(6)−B(2)−B(3)	113.1(3)	116.0(2)	113.8(2)	114.0(3)
B(6)−B(2)−B(5)	62.8(2)	62.0(2)	62.8(2)	62.4(2)
B(7)−B(2)−B(1)	113.5(3)	114.0(2)	113.5(2)	113.5(3)
B(7)−B(2)−B(3)	62.2(2)	64.3(2)	62.6(2)	62.8(2)
B(7)−B(2)−B(5)	114.3(3)	114.6(2)	113.8(2)	113.9(3)
B(7)−B(2)−B(6)	62.4(2)	63.4(2)	62.1(2)	62.4(2)
B(2)−B(3)−B(1)	59.1(2)	60.1(2)	59.2(2)	59.3(3)
B(7)−B(3)−B(1)	108.4(3)	107.6(2)	108.0(2)	108.1(2)
B(7)−B(3)−B(2)	58.2(2)	57.1(2)	58.3(2)	58.3(2)
S/B(8)−B(3)−B(1)	114.5(3)	113.5(2)	114.6(2)	113.6(2)
S/B(8)−B(3)−B(2)	109.7(2)	108.0(2)	109.4(2)	109.6(2)
S/B(8)−B(3)−B(7)	62.1(1)	60.6(2)	60.9(2)	61.7(2)
B(9)−B(3)−B(1)	61.4(2)	59.7(2)	61.0(2)	61.1(2)
B(9)−B(3)−B(2)	103.6(3)	102.4(2)	103.0(2)	103.2(2)
B(9)−B(3)−B(7)	105.0(3)	103.3(2)	103.6(2)	103.7(3)
B(9)−B(3)−S/B(8)	60.6(2)	61.3(2)	61.0(2)	59.8(2)
B(5)−S/B(4)−B(1)	56.6(2)	59.5(2)	57.0(2)	57.7(2)
B(9)−S/B(4)−B(1)	58.9(2)	57.3(2)	58.7(2)	59.4(2)
B(9)−S/B(4)−B(5)	99.2(2)	98.7(2)	99.0(2)	100.5(2)
B(2)−B(5)−B(1)	59.3(2)	58.9(2)	59.3(2)	58.9(2)
S/B(4)−B(5)−B(1)	61.2(2)	60.5(2)	61.3(2)	60.6(2)
S/B(4)−B(5)−B(2)	109.9(3)	111.8(2)	110.5(2)	109.2(2)
B(6)−B(5)−B(1)	108.4(3)	108.4(2)	108.7(2)	108.0(2)
B(6)−B(5)−B(2)	59.0(2)	59.1(2)	59.2(2)	58.9(2)
B(6)−B(5)−S/B(4)	113.3(3)	118.8(2)	114.3(2)	113.5(2)
B(5)−B(6)−B(2)	58.2(2)	59.0(2)	58.0(2)	58.7(2)
B(7)−B(6)−B(2)	58.7(2)	57.1(2)	58.7(2)	58.7(2)
B(7)−B(6)−B(5)	107.4(3)	106.9(2)	107.1(2)	107.8(3)
B(3)−B(7)−B(2)	59.6(2)	58.6(2)	59.1(2)	58.9(2)
B(6)−B(7)−B(2)	58.8(2)	59.5(2)	59.2(2)	58.9(2)
B(6)−B(7)−B(3)	108.1(3)	108.2(2)	108.6(2)	108.0(2)
S/B(8)−B(7)−B(2)	109.4(3)	110.5(2)	110.0(2)	109.2(2)
S/B(8)−B(7)−B(3)	60.3(2)	62.2(2)	60.8(2)	60.6(2)
S/B(8)−B(7)−B(6)	112.8(3)	113.7(2)	114.7(2)	113.5(2)
B(7)−S/B(8)−B(3)	57.7(2)	57.2(2)	58.3(2)	57.7(2)
B(9)−S/B(8)−B(3)	58.8(2)	57.9(2)	59.2(2)	59.4(2)
B(9)−S/B(8)−B(7)	100.5(2)	98.4(2)	100.4(2)	100.5(2)
B(3)−B(9)−B(1)	58.3(2)	57.3(2)	58.0(2)	57.9(2)
S/B(4)−B(9)−B(1)	61.8(2)	58.3(2)	61.0(2)	60.8(2)
S/B(4)−B(9)−B(3)	113.0(3)	109.9(2)	112.1(2)	111.7(3)
S/B(8)−B(9)−B(1)	111.8(3)	111.0(2)	110.9(2)	111.7(3)
S/B(8)−B(9)−B(3)	60.6(2)	60.8(2)	59.8(2)	60.8(2)
S/B(8)−B(9)−S/B(4)	124.5(2)	126.7(2)	125.1(2)	124.7(3)

[a] S/B(4) and S/B(8) refer to mixed boron−sulfur sites which result from a 50/50 disorder of a sulfur atom over the cluster 4- and 8-positions. [b] Angles for subcluster a. [c] Angles for subcluster b. [d] B(1)−B(3), S/B(4)−S/B(8),a nd B(5)−B(7) pairs are related by a mirror plane at $y = ^1/_4$.

Table 6. Selected Exocluster Bond Distances (pm) and Angles (deg) for *exo*-6-L-*arachno*-4-SB_8H_{10} Compounds [L = uro (**2f**), $^1/_2$ uro (**2g**), MeNC (**2h**)]

Compound **2f**			
C(12)−N(1)	152.5(5)	C(13)−N(1)	152.8(5)
C(14)−N(1)	152.3(5)	B(6)−N(1)	159.3(5)
C(13)−N(1)−C(12)	106.5(2)	C(14)−N(1)−C(12)	107.6(3)
C(14)−N(1)−C(13)	107.4(3)	B(6)−N(1)−C(12)	108.4(3)
B(6)−N(1)−C(13)	109.8(3)	B(6)−N(1)−C(14)	116.7(2)
Compound **2g**			
C(12)−N(1)	148.1(2)	C(12)−N(2)	148.1(2)
C(13)−N(1)	151.9(3)	C(23)−N(2)	152.6(3)
C(14)−N(1)	153.3(3)	C(24)−N(2)	153.1(3)
B(6a)−N(1)	162.0(3)	B(6b)−N(2)	160.1(4)
C(13)−N(1)−C(12)	108.4(2)	C(23)−N(2)−C(12)	107.8(2)
C(14)−N(1)−C(12)	107.8(2)	C(24)−N(2)−C(12)	108.4(2)
C(14)−N(1)−C(13)	107.0(2)	C(24)−N(2)−C(23)	106.8(2)
B(6a)−N(1)−C(12)	112.6(2)	B(6b)−N(2)−C(12)	113.7(2)
B(6a)−N(1)−C(13)	112.7(2)	B(6b)−N(2)−C(23)	110.2(2)
B(6a)−N(1)−C(14)	108.1(2)	B(6b)−N(2)−C(24)	109.7(2)
B(2a)−B(6a)−N(1)	115.7(2)	B(2b)−B(6b)−N(2)	116.6(2)
B(5a)−B(6a)−N(1)	116.8(2)	B(5b)−B(6b)−N(2)	119.1(2)
B(7a)−B(6a)−N(1)	119.9(2)	B(7b)−B(6b)−N(2)	118.8(2)
Compound **2h**			
N(6)−C(6)	114.2(4)	C(61)−N(6)	143.1(5)
C(6)−B(6)	153.7(6)		
C(6)−B(6)−B(2)	109.2(3)	C(6)−B(6)−B(5)	115.7(2)
N(6)−C(6)−B(6)	179.8(1)	C(61)−N(6)−C(6)	178.8(3)
B(2)−B(6)−C/N(1)	118.9(3)	115.7(2)	116.6(2)	109.2(3)
B(5)−B(6)−C/N(1)	118.5(3)	116.8(2)	119.1(2)	115.7(2)
B(7)−B(6)−C/N(1)	120.9(3)	119.9(2)	118.8(2)	115.7(2)

principally differential crystal-packing forces about the two different subclusters, but the mean values approximate closely those for the monodentate species **2f**. The mean interboron distances for the undisordered cage atoms compare well with the corresponding distances in other, ordered, nine-vertex *arachno* clusters.[21]

The ligand-to-cage C(6)−B(6) distance of 153.7(6) pm for compound **2h** approximates to that typical for a carbon−boron 2-electron 2-center single bond,[22] and the C(6)−N(6) distance of 114.2(4) pm suggests that the essence of the triple-bond character of the MeCN ligand has been preserved. The C(6)−B(6)−B(2) and H(6)−B(6)−C(6) interatomic angles for compound **2h**, at 109.3(3) and 111.2(5)°, respectively, indicate an almost regular tetrahedral disposition of the bonding to the *exo* ligand and the *endo* hydrogen atom around the substituted B(6) atom. On the other hand, the corresponding angles for the urotropine compounds **2f** and **2g** [119.5(3) and 104.7(16)° for **2f** and 116.0 (mean) and 107.3° (mean) for **2g**] suggest a tetrahedral environment somewhat more distorted from the regular.

For the urotropine cages in compounds **2f** and **2g**, the angles around the N(1) center in **2f** (mean 109.4°) approximate well to an idealized tetrahedral arrangement, as do the corresponding angles about the N(1) and N(2) atoms in compound **2g** (mean 109.41°). N-Substitution by the thiaborane moieties on the urotropine cages of both **2f** and **2g** brings about significant lengthening of the N(subst)−C distances, the mean values being 152.4 and 151.2 pm, respectively, in comparison with the other sets of nitrogen−carbon distances which have mean values of 146.4 and 145.6 pm, respectively. This lengthening is consistent with the relatively strong electron-donating effect on the $\{4\text{-}SB_8H_{10}\}$ subcluster(s) concomitant with the nitrogen quarternization.

Mass Spectrometry. The mass spectra of the ligand derivatives of type **2** (see Experimental Section and Table 1) exhibited the expected molecular ion peaks and showed principal fragmentations to give $[SB_8H_{10}]$, this fragmentation being particu-

---

(21) (a) Plešek, J.; Štíbr, B.; Fontaine, X. L. R.; Jelínek, T.; Thornton-Pett, M.; Heřmánek, S.; Kennedy, J. D. *Inorg. Chem.*, in press. (b) Voet, D.; Lipscomb, W. N. *Inorg. Chem.* **1967**, *6*, 113.

(22) Beaudet, R. A. In *Advances in Boron and the Boranes*; Liebman, J. E., Greenberg, A., Williams, R. E., Eds.; VCH Publishers: New York, 1988; pp 417−490 and references therein.

Table 7. ^{11}B and ^1H Chemical Shifts for *exo*-6-L-*arachno*-4-SB_8H_{10} Compounds (**2**) in $CDCl_3$ at 294−297 K

	$\delta(^{11}B)$[a] ($^1J(^{11}B-^1H)$, Hz) [$\delta(^1H)$[a]]									
compd	BH(9)	BH(5)	BH(7)	BH(2)	BH(8)	BH(1)	BH(6)[b]	BH(3)	H(8,9)	H(7,8)
2a	4.8	−0.4	−4.6	−4.6	−27.0	−28.9	−32.8	−48.5		
	(154)	(155)	(150)[c]	(150)[c]	(165)	(180)[c]	(128)	(148)		
	[3.50]	[3.11]	[2.54]	[2.52]	[1.80]	[1.53]	[0.24]	[0.15]	[−0.63]	[−3.56]
2b	5.3	1.2	−2.5	−6.6	−26.8	−27.8	−46.4	−48.0		
	d	(138)	(139)	(137)	(142)[c]	(150)	*d, e*	(148)		
	[3.56]	[3.16]	[2.57]	[2.13]	[1.86]	[1.53]	[−0.18]	[−0.21]	[−0.42]	[−2.59]
2c	4.2	0.9	−2.6	−5.0	−27.3	−29.2	−37.4	−48.8		
	(155)	(154)	(143)	(142)	(149)	(179)[c]	(128)	(148)		
	[3.43]	[3.18]	[2.59]	[2.53]	[1.75]	[1.51]	[0.47]	[0.13]	[−0.74]	[−3.07]
2d	5.0	−0.5	−5.6	−7.4	−28.4	−30.9	−20.4	−48.3		
	(155)	(150)	(138)	(137)	(152)	(173)[c]	(126)	(147)		
	[3.54]	[3.10]	[2.42]	[2.64]	[1.68]	[1.41]	[0.62]	[0.19]	[−0.74]	[−3.12]
2e	4.7	1.2	−3.4	−5.0	28.0	−29.9	−24.6	−48.0		
	(155)	(156)	(150)[c]	(150)[c]	(155)	(186)	(117)	(147)		
	[3.57]	[3.26]	[2.64]	[2.66]	[1.75]	[1.53]	[1.46]	[0.24]	[−0.56]	[−2.82]
2f	5.2	−1.6	−6.4	−8.9	−28.1	−30.6	−26.5	−48.7		
	(153)	(148)	(134)	(134)	(158)[c]	(176)	(130)[c]	(148)		
	[3.54]	[3.13]	[2.47]	[2.46]	[1.71]	[1.48]	[−0.09]	[0.18]	[−0.76]	[−3.22]
2g	5.0	−2.0	−6.2	−8.3	−27.6	−30.3	−25.4	−48.9		
	(150)	(147)	(133)	(134)	(138)[c]	(175)	(150)[c]	(150)		
	[3.53]	[3.13]	[2.51]	[2.59]	[1.77]	[1.51]	[0.07]	[0.18]	[−0.75]	[−3.25]
2h	4.4	1.5	−1.8	−6.7	−27.8	−26.9	−54.2	−49.0		
	(155)	(157)	(146)	(142)	(152)	(140)[c]	(120)	(149)		
	[3.56]	[3.25]	[2.72]	[2.41]	[1.65]	[1.88]	[−0.78]	[0.13]	[−0.70]	[−2.87]
2i	5.0	1.0	−2.8	−4.3	−27.8	−29.7	−26.9	−47.8		
	(157)	(150)	(190)[c]	(151)[c]	(150)[c]	(180)[c]	*c*	(148)		
	[3.63]	[3.28]	[2.66]	[2.80]	[1.82]	[1.53]	[1.65]	[0.23]	[−0.39]	[−2.57]

[a] Assignment by relative intensities; [$^{11}B-^{11}B$] COSY (measured for all compounds; observed cross-peaks 1−2 s, 1−3 s, 1−5 w, 1−9 w, 2−3 s, 2−5 s, 2−6 s, 2−7 s, 3−7 s, 3−8 s, 3−9 s; s = strong, w = weak) and $^1H\{^{11}B(selective)\}$ experiments (for ^1H). [b] Signals of the *endo* hydrogen atoms. Additional signals of the exoskeletal ligand: **2a**, 2.44 (s, 6H, SMe_2); **2b**, *ca.* 7.56 (center) (m, 15H, PPh_3); **2c**, 2.12 (s, 3H, MeCN); **2d**, 2.80 (s, 9H, NMe_3); **2e**, 9.78−7.60 (m, 5H, py); **2f**, 4.70−4.36 (m, 12H, uro); **2g**, 4.80−4.20 (m, 12H, uro); **2h**, 3.56 (s, 3H, MeNC); **2i**, 9.0−7.3 (m, 7H, quin). [c] Value uncertain due to peak overlap. [d] Broad signal, $^1J(^{11}B-^1H)$ cannot be defined. [e] $^1J(^{11}B-^{31}P)$ = ca. 117 Hz.

larly marked for the SMe_2 and MeCN compounds **2a** and **2h**. In fact, for compound **2a**, the molecular ion was very weak under 70-eV electron-impact ionization conditions, and for compound **2b**, it was not observed. Under fast-atom bombardment ionization, however, the molecular ions for both these species were more readily observed. This is consistent with the general trends of ligand affinities for boron centers in polyhedral boron-containing compounds.

NMR Spectroscopy. All compounds were examined by NMR spectroscopy to confirm bulk purity, to measure and assign the observed resonances, and to confirm the molecular formulation. ^{11}B and ^1H NMR spectroscopy, making use of the [$^{11}B-^{11}B$] COSY[23] (for characteristic cross-peaks see Table 7) and $^1H\{^{11}B(selective)\}$ techniques,[24] resulted in the complete assignment of all the ^1H and ^{11}B resonances for compounds of type **2**. The measured data for this series of new nine-vertex *arachno* thiaboranes are in Table 7, and illustrative aspects of the ^{11}B and ^1H shielding behavior are presented graphically in Figures 4 and 5.

The NMR data for all the compounds **2a**−**h** are entirely consistent with the general constitution **2** and also with the results of the X-ray diffraction studies (see Figures 1−3) and mass spectrometry. Intercomparison of the ^{11}B shielding patterns (lower parts of Figures 4 and 5) reveals very similar shielding behaviors for all the compounds. Although there are significant differences for the ligand-substituted B(6) sites, the long-range substituent effects are very small, and there are only trivial differences in chemical shift and (sometimes) in the corresponding ordering among closely spaced resonances for the other sites. The individual $\{\delta(^{11}B),\delta(^1H)\}$ data points for all the compounds of type **2** (Figures 4 and 5 uppermost diagrams) all fall close to a single $\delta(^{11}B):\delta(^1H)$ correlation line, except of course those for the more highly shielded ^1H(*endo*-6) position, as found also for the isostructural carborane analogs *exo*-6-L-*arachno*-4-CB_8H_{12} (structure **6**; see Chart 1).[21a] As expected, intercomparison of the ^{11}B and ^1H shielding patterns for equivalent compounds in the two isostructural series consisting of the thiaboranes of structure **2** and the carboranes of structure **6** reveals a marked similarity between most of the ^{11}B and ^1H resonances for corresponding positions.

Concluding Remarks

The simple reactions outlined in this paper, involving the readily available thiaboranes such as 4-SB_8H_{12}[8] and 6-SB_9H_{11}[11] as starting materials, have led to the isolation of members of the new subfamily of the general set of heteroborane-ligand adducts *exo*-6-L-*arachno*-4-EB_8H_{10}, where E is a main-group hetero atomic unit. The comparatively high stabilities of these new thiaboranes, together with the stabilities of their carbaborane analogs (E = CH_2),[21a] suggest that other structurally related stable species, e.g. azaborane analogues or cage and positional isomers, may also be synthesizable and stable. In any event, the new thiaboranes are expected to exhibit interesting chemical behavior and, also, thereby generate other novel thiaborane species, such as the recently reported [*nido*-9-SB_8H_9]$^-$ anion,[25] and we are currently examining aspects of this possibility.

Acknowledgment. The authors thank the Academy of Sciences of the Czech Republic (Grants 43203 and 432402), the U.K. SERC (Grants F43215 and F78323), the Royal Society

---

(23) Hutton, W. C.; Venable, T. L.; Grimes, R. N. *J. Am. Chem. Soc.* **1984**, *106*, 29.

(24) Fontaine, X. L. R.; Kennedy, J. D. *J. Chem. Soc., Dalton Trans.* **1987**, 1573.

(25) Holub, J.; Štíbr, B.; Kennedy, J. D. *Collect. Czech. Chem. Commun.*, in press.

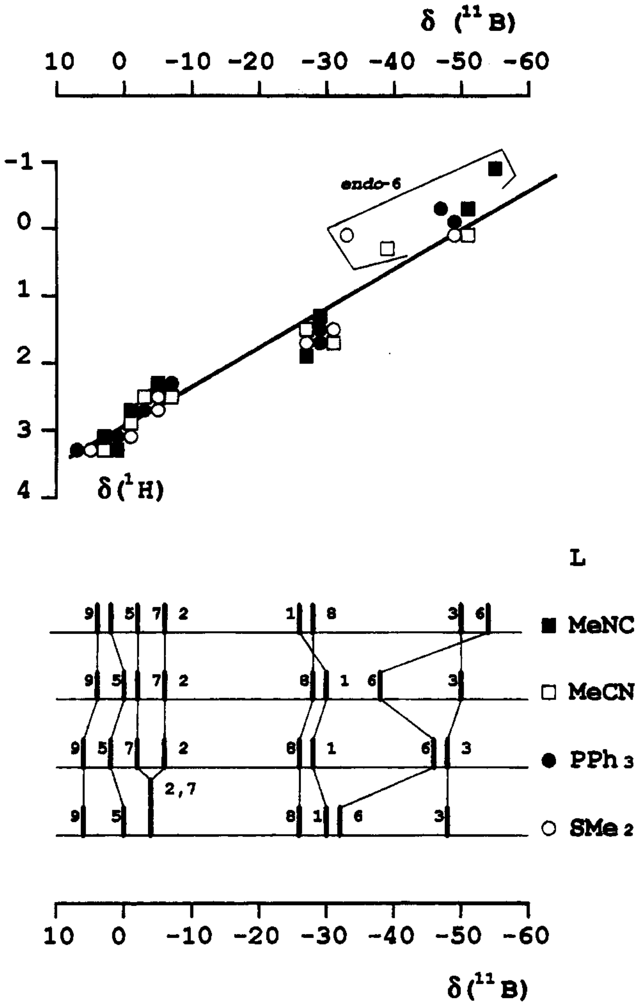

Figure 4. Upper diagram: Plot of δ(^{1}H) versus δ(^{11}B) for the thiaboranes *exo*-6-L-*arachno*-4-SB_8H_{10} [L = SMe_2 (**2a**, ○), PPh_3 (**2b**, ●), MeCN (**2c**, □), MeNC (**2h**, ■)]. The line drawn has a slope δ(^{1}H)/δ(^{11}B) *ca.* 1:17.5 and intercept +3.0 ppm in δ(^{1}H).

(London), and Borax Research Ltd. (Chessington, U.K.) for support and Dr. T. S. Griffin and Dr. D. M. Wagnerová for their helpful interest. We also thank Dr. Z. Weidenhoffer and Mr. D. Singh for mass spectrometric measurements.

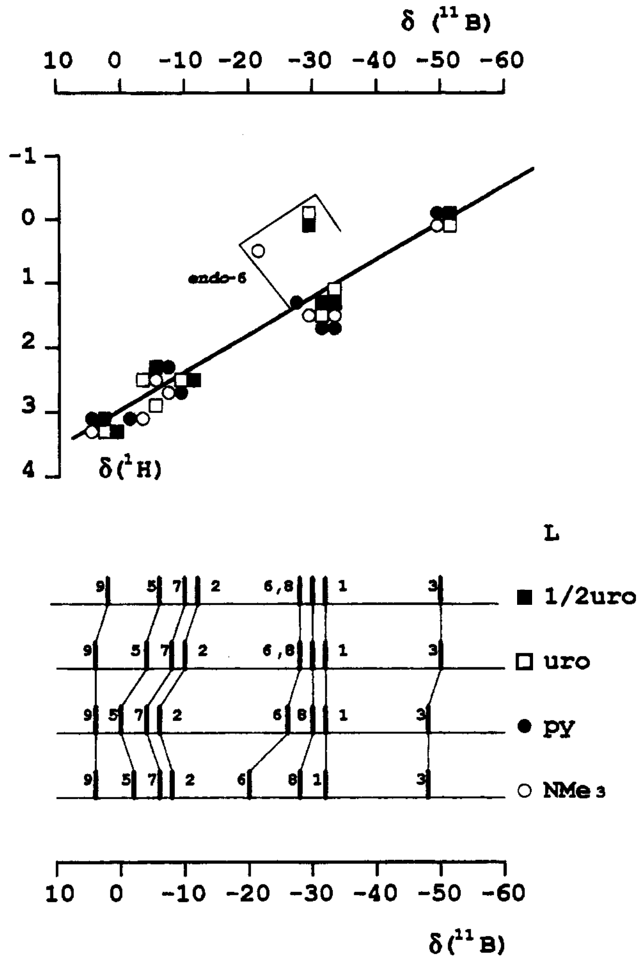

Figure 5. Upper diagram: Plot of δ(^{1}H) versus δ(^{11}B) for the thiaboranes *exo*-6-L-*arachno*-4-SB_8H_{10} [L = NMe_3 (**2d**, ○), py (**2e**, ●; compound **2i** exhibits very similar NMR patterns), uro (**2f**, □), and $^{1}/_{2}$ uro (**2g**, ■)]. The line drawn has a slope δ(^{1}H)/δ(^{11}B) *ca.* 1:17 and intercept +3.0 ppm in δ(^{1}H).

Supplementary Material Available: Tables giving data collection parameters, positional parameters for the hydrogen atoms, anisotropic thermal parameters, and complete interatomic distances and bond angles for compounds **2g** and **2h** (13 pages). Ordering information is given on any current masthead page.